Materials Research Proceedings 54 (2025) 30-38 https://doi.org/10.21741/9781644903599-4

Modeling the filament of magnesium alloys

Bruni Carlo

Università Politecnica delle Marche - DIISM, Via Brecce Bianche, 60131 Ancona, Italy

c.bruni@univpm.it

Keywords: FDM, Modeling, Magnesium Alloy

Abstract. The realization of the required geometry when representing the complex part of an object is determined by discretization of the material amount to be applied by a filament. The FDM of metals could in this way be competitive with conventional technologies to net shape making. The possibility to realize smaller and smaller filaments whose characteristics can be given in the extruding tool-material system by using proper geometries and parameters in order to produce the temperature rise inside the container is investigated. The analytical modeling proposed describes the extrusion behaviour of two magnesium alloys, that are the AZ31 and the ZM21 ones. That to perform a filament section of 0.4-0.5 mm in radius, beginning by a one of about 1.5 mm, with which to apply metal ribs. The effect of friction, distortion and heating phenomena as well as the solid fraction are considered on the stress vs. displacement curves inside the extruder until submillimeter diameter. The material model updated to consider the higher strain rates evidences the different behaviour of the models in describing different strain rates conditions useful to realize the filament geometry.

Introduction

Casting technologies for realization of products as reported in scientific literature [1] require high pressure [2] to get the component with the required geometry avoiding as much as possible machining operations. A similar method can be applied when the bulk metal fabrication of components or parts of them is used. The knowledge of the materials in terms of the models describing their behaviour when deformed in order get the desired shape [3,4,5] is required. In most of cases the fabrication can be done by using conventional in temperature stamping methods subdivided in different phases to perform uniform deformations on workpiece. But, the complex shapes of the object to be made can be realized by additive manufacturing methods [6-8] based on hot arc forging, laser wire feed and laser direct energy deposition by which it could be entirely fabricated. Among the additive manufacturing technologies the FDM (Fused Deposition Modeling) of metals represents the most useful way to integrate the traditional manufacturing with the approach of additive manufacturing in working material [9-11]. The competitiveness of such technology is effectively represented when the complexity characterizes all of the object. But it could be too time expensive when the design stage is not thought on surface of that. The FDM [12,13] by this way can be tuned and used to get filament depositions realizing parts of objects already fabricated with simple shaped tools in conventional forging or stamping ways. The added part may be then fine tuned depending on the filament section and the final configuration reached with other surface treatments in order to get also the required finish. Anyway, the discretization of the material deposition determines the achievement of the precision in the rib application. But the key variable of the process is represented by the temperature of the material at extruder exit determining the conditions of the filament in terms of its geometry and of solid-liquid fraction [14]. The temperature inside the extruder is obtained by setting that to the value imposed to the tool material system plus the increase due to heating phenomena [13]. Such conditions are more time variant in other systems such as metal powder jetting and direct fusion filament [8, 15,16] technologies in which the heat generated is supplied directly by the spot on the surface to be

liquified even if some effects of shielding can appear. Anyway in FDM the material undergoes different stages in terms of heating, deformation and partial phase transition determining some delays in supplying material at predicted conditions at the surface of the object to be completed with respect to cold systems [17,18]. The author in previous work [13] reported the effect of heating phenomena in reaching the temperatures able to supply material in the due condition to be applied using analytical modeling based on friction slab method.

In general the study of extrusion base additive manufacturing techniques in particular for some kinds of magnesium alloys does not take into consideration the different heating contributions such as friction and distortion determining the final condition and the level of solid fraction reached. Such variables are particularly sensitive when at the under millimeter levels.

The present paper aims at studying the effect of the different variables affecting heating generation on two magnesium AZ31 and ZM21 alloys under extruding condition to realize ribs to be applied on planar surfaces. By the proposed extruding analytical modeling the already mentioned variables are considered and the stress amount with related temperature increase evaluated in order to reach the desired filament section. A method to check the obtained results at solid and semisolid also in terms of material modeling is reported for different conditions of strain rates.

Modeling

The procedure proposed and reported in Fig. 1 whose details will explained in the following consists in the building and in the using of an analytical model of extrusion considering the slab method applied when the semiconical angle α approaches 90°. Under that condition material flow is considered to get the 45° angle under high temperatures at solid state. That is the conical part of the tool. The quantification of stress amount due to the variables reported in the following allows the heating calculation depending on friction and distortion effects. By those computations the solid/liquid fraction can be evaluated and stress orders of magnitude analytically detected and related to the rib section deposition. To check the obtained results at solid and semisolid also in terms of material modeling the stress amounts in different conditions of strain rates are compared for two different alloys being related to the filament section reached.

At the millimeter order of magnitude the effect of heating from the tuned temperature is reported by the author in previous researches [13] using the friction based slab method.

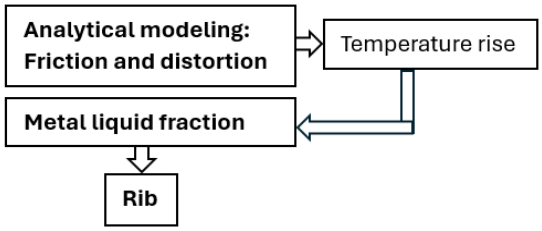

Figure 1 – Modeling.

At the millimiter-submillimeter threshold the extruding behaviour of two magnesium alloys named AZ31 and ZM21 is described considering the material flow of pure deformation (without friction and distortion) reported in the following with that related to the cylindrical zone:

$$\sigma_z = \frac{2\cdot\bar{\sigma}\cdot\ln\left(\frac{R_0}{R_f}\right)R_0^2}{R_f(2\cdot R_0 - R_f)} \quad (1)$$

$$\sigma = \sigma_z \cdot exp\left(\frac{2\mu}{R_0}\Delta l\right) \quad (2)$$

where:

- σ_z: extrusion tension
- $\overline{\sigma}$:material flow
- μ: friction coefficient
- R_0: initial billet radius
- R_f :final billet radius
- σ: tension at the stem of the container
- Δl: travel covered by the stem

The constitutive equations supplied and summarized by the author in [13] are useful for the strain rate interval reported in [19,20] for the AZ31 and ZM21 magnesium alloys in order to describe their in temperature behaviour. But when the strain rate increases what described in the just reported references produces too much high stress levels in particular for ZM21. Under these conditions the equation describing the behaviour of two magnesium alloys in particular for ZM is adapted to avoid variables in which the strain rate determines a too much high contribution to the stress. Really an acceptable augmentation in stress of material with increasing deformation velocity can be probably due to the Manganese amount that determines some increase in strength with high strain rate with a order of magnitude of tens [21,22].
In detail being the same the constitutive equation already proposed for AZ31 and reported by the author in [13,19,20] and represented as follows:

$$\bar{\sigma} = \mathrm{k}\, \varepsilon^n \dot{\varepsilon}^m. \tag{3}$$

An updated one with respect to [13,19] in the modeling of ZM21 is proposed by the following equation:

$$\bar{\sigma} = \beta_1 \varepsilon + \beta_2 \ln(\dot{\varepsilon}) + \beta_3 T^2 + \beta_6 \varepsilon^2 \tag{4}$$

being:

- ε: deformation;
- $\dot{\varepsilon}$: strain rate.

The material coefficients depending on temperature K, n, m and β_1 , β_2 , β_3 and β_6 constants are reported in [19,20].

Concerning the increase in temperature due to the deformation and friction the following equations given by heat balancing are used:

$$\Delta T_{def} = \frac{\beta \bar{\sigma} \overline{\Delta \varepsilon}}{\rho c} \tag{5}$$

$$\Delta T_{fric} = \frac{\tau 2\pi R_0 l \cdot v \cdot t}{\rho V c} + \frac{\tau \pi (R_0^2 - R_f^2) \cdot (R_0 - R_f) \sqrt{\frac{tg\alpha^2 + 1}{tg\alpha^2}}}{\rho V c} \tag{6}$$

being:

- v: stem velocity
- ρ: density of material
- c: specific heat
- V: volume of the material
- ΔT: temperature increment

The shear stress τ is calculated as a function of normal to the container stress σ_y as that used in modeling of chip mechanics with the costant K equal to 0.08 in the cylindrical and in the under

deforming zone. The entire contribution beginning by the initial τ value (τ_0) at tuned temperature is represented by the following equation:

$$\tau = \tau_0 + K\sigma_y \quad (7)$$

The extrusion is studied considering the scheme of a initial billet with 1.5 mm in radius to a dimension of 0.5 mm with a extrusion chamber of about 11 mm in length. To determine the effect of the deformation at the near micro-extrusion configuration also a radius of 0.4 mm is considered.

The contribution of friction and of distortion are implemented to Eq. 1 considering an amount of 0.2 and 0.3 respectively. At the mean and at the best a solid fraction amounts from 0.5 to 0.1 are tuned to consider the stress levels as found for similar alloys behaviour at those temperature [3]. The filament section conditions for rib deposition are obtained.

The stress trend is subsequently evaluated under solid and semisolid state at strain rates of 5 and 40 1/s for modeling checking.

Results and discussion of analytical modeling

The thermal conditions of the extruding-material system in order to get the semisolid of the filament to be applied as ribs over a flat surface can be defined in terms of temperature reached by the material inside the extruder with a given tuned initial temperature. As shown in the next the tension behaviour is reported for both the materials at initial temperature of 400°C at strain rates up to a magnitude of tens.

Fig. 2 shows the decrease in stress with increasing displacement in the cylindrical part of the extruder due to friction contribution reduction. Then an increase at the final due to the deformation concentration until 0.5 mm in radius for both the alloys investigated. The second effect described by Eq. 1 and the other by Eq. 2. The results observed due to the material behaviour described by Eq. 3 and Eq. 4 do not take into consideration the friction, the distortion in the under deforming zone as well as the effect of solid fraction. In other words the plain condition.

Fig. 3 shows the increase of the tensional state due to friction considered by adding 0.2 to the sigma level as a contribution to the stress in the Eq. 1.

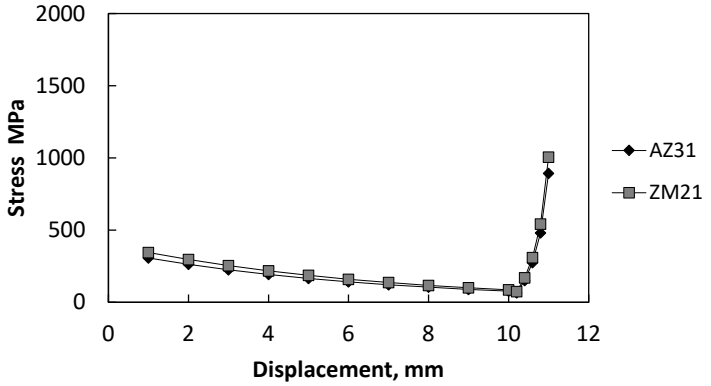

Figure 2 – Stress values of AZ31 and ZM21 without friction, distortion and solid fraction.

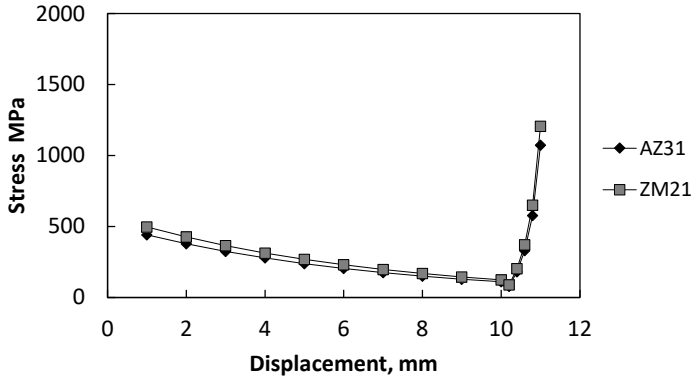

Figure 3 – Stress values of AZ31 and ZM21 with friction.

Fig. 4 reports the contribution of the distortion to the stress of Eq. 1 while Fig. 5 that of both friction and distortion on the extruding behaviour of the two alloys investigated to 0.5 mm and to 0.4 mm in radius of the exit filament. Of course an increase in stress can be observed for AZ31 and ZM21 magnesium alloys. The increase in temperature calculated with Eq. 5 and Eq. 6 and revealed in Fig. 6 and Fig. 7 for both the alloys at the cylindrical and at the under deforming zone allows to reach the conditions of semisolid useful for filament generation and rib application.

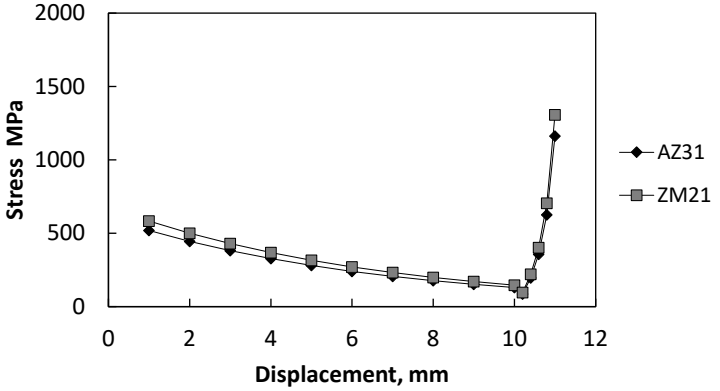

Figure 4 – Stress values of AZ31 and ZM21 with distortion.

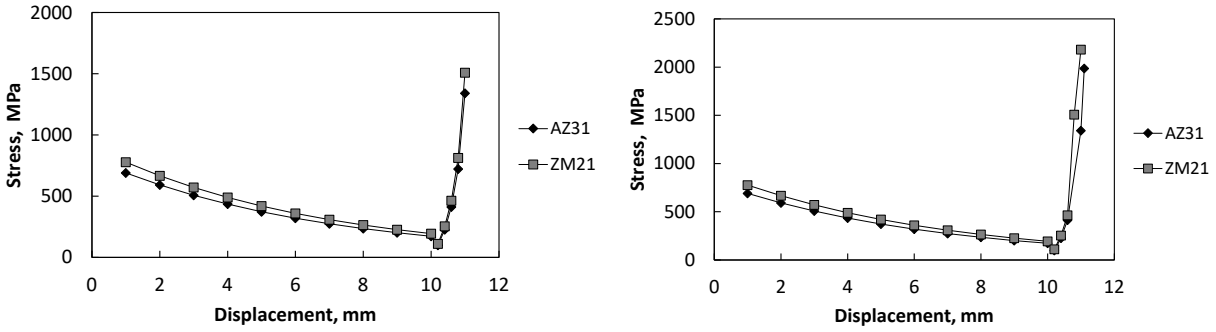

a) b)

Figure 5 – Stress values of AZ31 and ZM21 with friction and distortion until 0.5 mm (a) and at 0.4 mm (b) in radius.

Eq. 7 is used to evaluate the current shear stress at the tool-material contact interface for temperature rising calculated by Eq. 6. Fig. 8 allows to show the stress field inside the extruder under the condition of 0.1 solid fraction.

Materials Research Proceedings 54 (2025) 30-38 https://doi.org/10.21741/9781644903599-4

The results of the maximum stress at each condition in terms of plain, friction, distortion and both for two different magnesium alloys and two different strain rates are reported in Fig. 9. About the last condition, one deformation rate is one order of magnitude higher than the other.

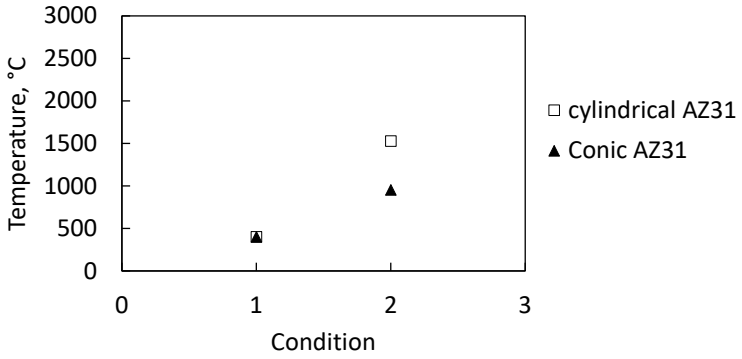

Figure 6 – Temperature values considering the plain condition: AZ31 alloy.

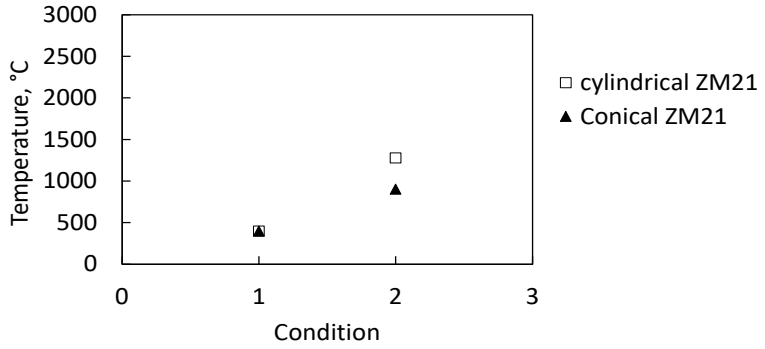

Figure 7 – Temperature values considering the plain condition: ZM21 alloy.

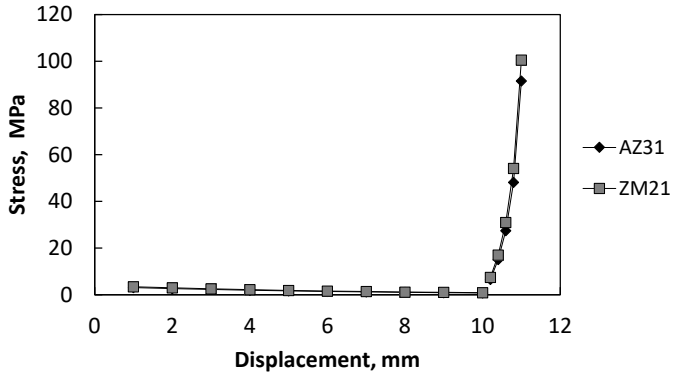

Figure 8 – Stress values at the plain condition: AZ31 and ZM21 alloy solid fraction of 0.1.

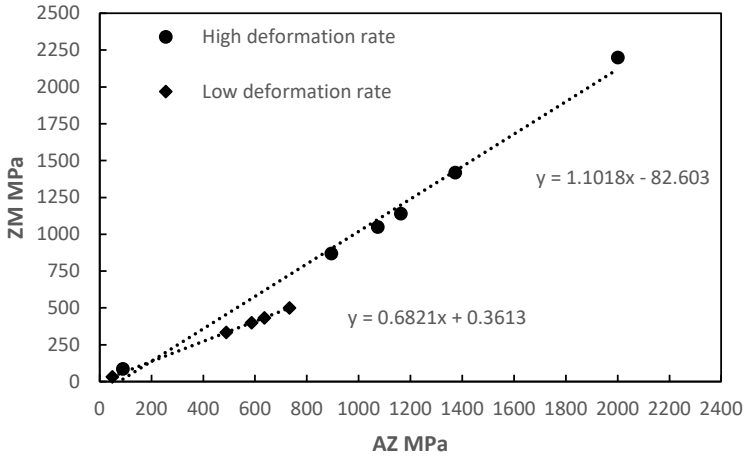

Figure 9 – Stress state of ZM vs. AZ magnesium alloys for different conditions: plain, with friction, with distortion, both of them and solid fractions of 0.5, 0.1 and 1.

This means that the constitutive equation proposed by the author and colleagues [13,19,20] modified to describe the ZM behaviour at high strain rate mainly not considering the variables containing the logarithmic function of $\dot{\varepsilon}$ and the $\dot{\varepsilon}^4$ to avoid a too much high hardening behaviour can be useful in describing the in temperature deformation. It is the Eq. 4. While no additional changes are made for that of AZ magnesium alloy. By this compensation the slope of ZM stress vs. AZ stress results remains anyway higher than the one at conventional testing strain rates. The results are in agreement with those reported by [22,23,24]. The resulting temperature increase under the plain condition seems to be enough to get the semisolid considering that only the mean values of the shear stress of Eq. 7 are taken for computing. The proposed methodology allows to adapt the scheme for a continuous extruding tool-material system for both the filament geometries of 0.5 and 0.4 mm in radius in which the steel stem function in a real operation could be performed by the cold solid magnesium alloy to be deformed as in the extrusion based by wire method.

Summary

The study of extruding base additive manufacturing system of two magnesium AZ31 and ZM21 alloys is performed proposing and applying a methodology based on a extrusion model. It is realized with slab method under the condition of planar tool and pure deformation with added effects of friction and distortion whose contribution allow to quantify the increase in stress inside the extruder. The modeling is made at the millimeter and sub-millimeter scale. The section of the realized filament to apply a rib got the 0.5 and 0.4 mm in radius. The increase in temperature evaluated considering the deformation contribution, the friction and the distortion using shear stress augmented by the normal stress for high pressure at the tool material contact surface allows to obtain values able to maintain the semisolid conditions with a mean solid fraction of 0.5 approximately reaching 0.1 under steady state. The material model updated in order to compensate too high hardening behaviours of previous ZM magnesium alloy model allows to detect the different stress conditions with two different strain rate behaviours differing from each other by one order of magnitude at least anyway useful for filament obtaining.

References

[1] Alan A. Luo. Magnesium casting technology for structural applications. Journal of Magnesium and Alloys 1 (2013) 2-22. https://doi.org/10.1016/j.jma.2013.02.002

[2] T. Li, J. Song, A. Zhang, G. You, Y. Yang, B. Jiang, X.Y. Qin, C. Xu, F. Pan, Progress and prospects in Mg-alloy super-sized high pressure die casting for automotive structural

components. Journal of Magnesium and Alloys 11 (2023) 4166-4180. https://doi.org/10.1016/j.jma.2023.11.003

[3] Q. Tang, M. Zhou, L. Fan, Y. Zhang, G. Quan, B. Liu, Constitutive behavior of AZ80 M magnesium alloy compressed at elevated temperature and containing a small fraction of liquid, Vacuum 155 (2018) 476-489. https://doi.org/10.1016/j.vacuum.2018.06.053

[4] W. Chen, W. He, B. Jiang, Q. Liu, F. Pan, Study on the compressive deformation behavior of a basal textured AZ31 magnesium alloy from the perspective of local strain, Materials Science & Engineering A 842 (2022) 143080. https://doi.org/10.1016/j.msea.2022.143080

[5] J. Chen, L. Rong, W. Wei, S. Wen, K. Gao, H. Huang, Z. Nie, An innovative thermal simulation study of microstructure improvement by delay forging during solidification, Journal of Materials Research and Technology 33 (2024) 4243-4252. https://doi.org/10.1016/j.jmrt.2024.10.122

[6] Huang, W., Chen, S., Xiao, J., Jiang, X., Jia, Y. Laser wire-feed metal additive manufacturing of the Al alloy. Opt. Laser Technol. (2021) 134, 10662. https://doi.org/10.1016/j.optlastec.2020.106627

[7] F. W. C. Farias, V. R. Duarte, I. Oliveira, J. da Cruz P. Filho, N. Schell, E. Maawad, J.A. Avila, J.Y. Li , Y. Zhang, G. Santos, J.P. Oliveira, In situ interlayer hot forging arc based directed energy deposition of Inconel® 625: process development and microstructure effects, Additive Manufacturing 66 (2023) 103476. https://doi.org/10.1016/j.addma.2023.103476

[8] L. E. S. Paes, H. Santos Ferreira, M. Pereira, F. A. Xavier, W. L. Weingaertner, L.O. Vilarinho, Modeling layer geometry in directed energy deposition with laser for additive manufacturing, Surface & Coatings Technology 409 (2021) 126-897. https://doi.org/10.1016/j.surfcoat.2021.126897

[9] A. I. Nurhudan, S. Supriadi, Y. Whulanza A. S. Saragih, Additive manufacturing of metallic based on extrusion process: A review. Journal of Manufacturing Processes 66 (2021) 228-237. https://doi.org/10.1016/j.jmapro.2021.04.018

[10] Y. Qi Li, F. Li, F. Wei Kang, H. Q. Du, Z. Y. Chen, Recent research and advances in extrusion forming of magnesium alloys: A review, Journal of Alloys and Compounds, 953 (2023) 170080. https://doi.org/10.1016/j.jallcom.2023.170080

[11] J. Feng, D. Zhang, H. Hu, Y. Zhao, X. Chen, B. Jiang, F. Pan, Improved microstructures of AZ31 magnesium alloy by semi-solid extrusion, Materials Science & Engineering A 800 (2021) 140204. https://doi.org/10.1016/j.msea.2020.140204

[12] M. Mousapour, M. Salmi, L. Klemettinen, J. Partanen, Feasibility study of producing multi-metal parts by Fused Filament Fabrication (FFF) technique, Journal of Manufacturing Processes 67 (2021) 438-446. https://doi.org/10.1016/j.jmapro.2021.05.021

[13] C. Bruni, Semisolid deposition of metallic material by extrusion-base analytical and simulative methodologies, Materials Research Proceedings 44 (2024) 433-44. https://doi.org/10.21741/9781644903254-47

[14] A. Jabbari and K. Abrinia, A metal additive manufacturing method: semi-solid metal extrusion and deposition, Int J Adv Manuf Technol (2018) 94:3819-3828. https://doi.org/10.1007/s00170-017-1058-7

[15] K. Andersen, Y. Dong and W. S. Kim, Highly conductive three-dimensional printing with low-melting metal alloy filament, Advanced engineering materials 19 (2017) 1700301. https://doi.org/10.1002/adem.201700301

[16] P. P. Selvam, S. Prabhakaran , B. Vinod , T. Jishnu. A review of energy efficiency and Machine learning analysis for additive manufacturing of direct laser metal deposition Materials Today: Proceedings.

[17] E. Navaneetha , A. A. Lakshmi, Cold extrusion on bulk materials: A review. Materials Today: Proceeding.

[18] C. O. Ufodike, G. C. Nzebuka. Investigation of thermal evolution and fluid flow in the hot-end of a material extrusion 3D Printer using melting model. Additive Manufacturing 49 (2022) 102502. https://doi.org/10.1016/j.addma.2021.102502

[19] C. Bruni, M. El Mehtedi, and F. Gabrielli, Flow curve modelling of a ZM21 magnesium alloy and finite element simulation in hot deformation, Key Engineering Materials Vols. 622-623 (2014) 588-595. https://doi.org/10.4028/www.scientific.net/KEM.622-623.588

[20] C. Bruni et al., Constitutive models for AZ31 Magnesium alloys, Key Engineering Materials, 367 (2008) 87-94. https://doi.org/10.4028/www.scientific.net/KEM.367.87

[21] C.L. Liu, X. Wang, N.C. Parson, W.J. Poole, The effect of Mn on the high temperature flow stress of Al-Mg-Si alloys, Materials Science & Engineering A 802 (2021) 140605. https://doi.org/10.1016/j.msea.2020.140605

[22] F. Zhang, Z. Liu, M. Yang, G. Su, R. Zhao, P. Mao, F. Wang, S. Sun, Microscopic mechanism exploration and constitutive equation construction for compression characteristics of AZ31-TD magnesium alloy at high strain rate, Materials Science and Engineering: A, 13 2020, 138571. https://doi.org/10.1016/j.msea.2019.138571

[23] X. Liu, B.W. Zhu, C. Xie, J. Zhang, C.P. Tang, Y.Q. Chen. Twinning, dynamic recrystallization, and crack in AZ31 magnesium alloy during high strain rate plane strain compression across a wide temperature. Materials Science & Engineering A 733 (2018) 98-107. https://doi.org/10.1016/j.msea.2018.07.030

[24] E.Kahana,A.B.-Artzy, O.Sadot, R.Z.Shneck, Microstructural evolution of AZ31 magnesium alloy after high strain rate expanding rings tests, Materials Science&Engineering A641 (2015) 274-280. https://doi.org/10.1016/j.msea.2015.06.054